

*Green Synthesis of Gold Nanoparticles Mediated by *Anastatica hierochuntica* Extract: Characterization and Evaluation of Their Physicochemical Properties*

Zainab A. Atea ^{1*}  and Asma G. Oraibi ²

^{1,2} Department of Plant Biotechnology, College of Biotechnology, Al-Nahrian University, Baghdad, Iraq

*Corresponding author: alizaenab794@gmail.com

Received: 31/5/2026 ,

Accepted: 18/6/2026,

Published: 30/6/2026.

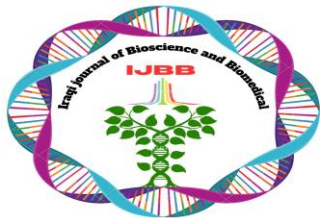


This work is licensed under a [Creative Commons Attribution 4.0 International License](https://creativecommons.org/licenses/by/4.0/)

Abstract

Green synthesis nanoparticles using *Anastatica hierochuntica* the whole-plant extract was used as a capping and stabilizing agent for the synthesis of gold nanoparticles. A hydrothermal process carried out between a plant extract and a one millimolar gold chloride precursor at a temperature of 45 degrees Celsius resulted in a fast color change to deep reddish-brown within 3 hours, indicating the kinetic reduction of trivalent gold ions. A strong Surface Plasmon Resonance absorption band at 490 nm was observed, confirming the formation of near-spherical nanostructures. Atomic Force Microscopy showed a marked topographical transformation, compressing the aggregates of the raw extract from an average diameter of 64.74 nm to about 42.23 nm in uniform nanoparticles. Field Emission Scanning Electron Microscopy (FE-SEM) has further supported this by showing distinct spherical structures of sizes 20.46-48.29 nm strongly immobilized in the porous organic template. The EDX spectra confirmed the presence of a carbonaceous matrix and indicated a three-fold increase in the chlorine concentration. Instrumental peak overlap at 2.12 keV further confirmed the encapsulation of macromolecular capping. From a mechanistic point of view, HPLC validated quantitatively the bioreduction pathway, showing a substantial post-synthesis reduction in all seven bioactive indices monitored. Gallic acid, for instance, reduced from 142.6 to 95.0 ppm, Rutin from 120.1 to 71.4 ppm, Luteolin, and p-coumaric acid by more than 50% of their initial values; these chromatographic reductions observed further confirm the role of native polyphenols and flavonoids as sacrificial electron donors in the reduction of gold ions. The rest of the fractions helped to create a stable steric barrier that hindered uncontrolled crystal growth and stopped particle agglomeration, leading to highly stable nanoparticles that can be used for advanced biomedical applications.

Keywords: Green synthesis, gold nanoparticles, *Anastatica hierochuntica*, physicochemical properties, HPLC.



Introduction

Nanotechnology is a field formed by the convergence of diverse disciplines of science, engineering, and technology that has allowed the generation of various types of functional nanoparticles (NPs) where at least one-dimension falls within the typical size range of 1-100 nm. Gold nanoparticles (AuNPs) are the most attractive metallic nanoparticles due to their unique surface plasmon resonance properties. They can be readily synthesized and their applications in medicine are well established. AuNPs can be synthesized by both chemical and physical means to achieve tunable size and multifunctional capability with well-characterized properties¹.

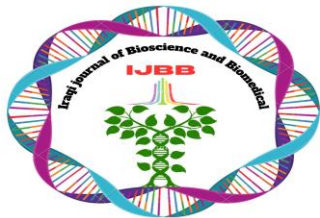
Metallic nanoparticles are defined as very small metal particles that measure between 1 nm and 100 nm. These are the elements that have been used in the synthesis of nanoparticles: silver (Ag), aluminum (Al), iron (Fe), gold (Au), silica (Si), copper (Cu), zinc (Zn), manganese (Mn), cerium (Ce), titanium (Ti), platinum (Pt), or thallium (TI). (NPs)².

The use of medicinal plants is as old as human history and much of modern medicine still relies on it. Many conventional drugs are plant-derived. Most of the few effective drugs a hundred years ago were plant-based. Aspirin, digoxin, quinine, morphine are some examples. Aspirin comes from willow bark; digoxin comes from foxglove; quinine comes from cinchona bark; morphine comes from the opium poppy. The development of drugs from plants is continuing. Pharmaceutical companies are involved with large scale pharmacological screening of herbs³.

Use of whole plants— Herbalists commonly use crude extracts of plants that may contain various constituents. They argue that these constituents can interact synergistically to give an overall effect of the entire herb greater than the sum of its individual parts. They also argue that using whole herbs reduces toxicity compared to isolated active ingredients, a concept they call "buffering." Practitioners claim that even though there might be some differences in the constituent compound ratios between two samples of a particular herbal drug, such variation does not usually lead to clinical issues. There is some experimental evidence in certain whole plant preparations supporting the ideas of synergy and buffering to some extent. However, to what extent these experimental findings can be generalized to all herbal formulations is not clear. herbal products are not known⁴.

Herb combining— Sometimes, a group of various herbs is employed together. Practitioners approach this with the philosophy of synergy and buffering between plant combinations, claiming that the efficacy and adverse reactions of the treatment can be reduced when herbal medicines are used in combination. This is in sharp contrast to conventional wisdom in medicine, where polypharmacy is generally "to be avoided at all costs," so to speak. possible⁵.

Green synthesis, the most economical biological route and environmentally benign process, has emerged as a prime approach for nanoparticle (NP) synthesis due to the use of low-cost and non-toxic raw materials. This sustainable method for NPs synthesis offers significant therapeutic efficacy, diminished toxicity, targeted binding, and site-specific applications. delivery⁶. Additionally, this does not affect human health and the environment, and are has been gaining interest by worldwide researchers⁷, that



exhibits the critical need for further development of antitumor therapeutic research, which has potential to target tumors and effectively kill cancer cells with very few side effects.

Anastatica is a monotypic genus, its type species being *Anastatica hierochuntica*. It belongs to the family Brassicaceae (formerly Cruciferae), placed under division Magnoliophyta and class Magnoliopsida⁸. The plant is a small gray annual herb, never exceeding 15 cm in height, with minute white flowers. It is a tumbleweed and a resurrection plant⁹.

The dry regions of the Middle East and the Sahara Desert in North Africa, Iran, Egypt, Palestine, Iraq, Jordan, and Pakistan are some of the places where *Anastatica* is found. Dieback is experienced by it after the rainy season when its leaves and branches dry up and curl into a tight ball. The fruits are enclosed within this formation and thus, the seeds cannot be dispersed as they are tightly secured and sealed prematurely¹⁰.

Curling and uncurling can be repeated indefinitely. This ability of the plant is due to its content of trehalose, a disaccharide that functions in many cryptobiosis-related mechanisms.

Medicinal plants are widely used in Hijaz, Najd, and Al Rub'Al Kali, and *Anastatica hierochuntica* is one of the most commonly used medicinal plants in these regions. Traditional medicine recommends the use of this plant for very serious health problems labor¹¹. uterine hemorrhage and to facilitates the expulsion of dead fetuses¹².

The German Commission E endorses *Anastatica* in the treatment of menstrual disorders, mastalgia, and premenstrual syndrome (PMS) [1]. It has been applied in the treatment of fibroid cysts and infertility (3), as well as for preventing miscarriages due to insufficient corpus luteum function and for postnatal placenta elimination. German health authorities recommend its use for corpus luteum insufficiency, menopausal symptoms, and inadequate milk production in nursing mothers. [10].¹³ It is used to treat acne in teenagers [11]. The whole dried plant contains flavonoids: Quercetin(flavonol), Luteolin (flavone)¹⁴.

Anastatica hierochuntica was selected as the biological reducing agent due to its rich phytochemical profile, particularly its abundance of phenolic compounds, flavonoids, tannins, and other antioxidant metabolites. These bioactive constituents contain functional groups capable of reducing Au³⁺ ions to elemental gold (Au⁰) while simultaneously acting as stabilizing and capping agents during nanoparticle formation. Previous studies have reported that *A. hierochuntica* possesses significant antioxidant activity and high total phenolic content, properties that are closely associated with efficient metal ion reduction in green nanoparticle synthesis. Furthermore, the plant is widely available in arid regions, making it an economical, sustainable, and environmentally friendly resource.

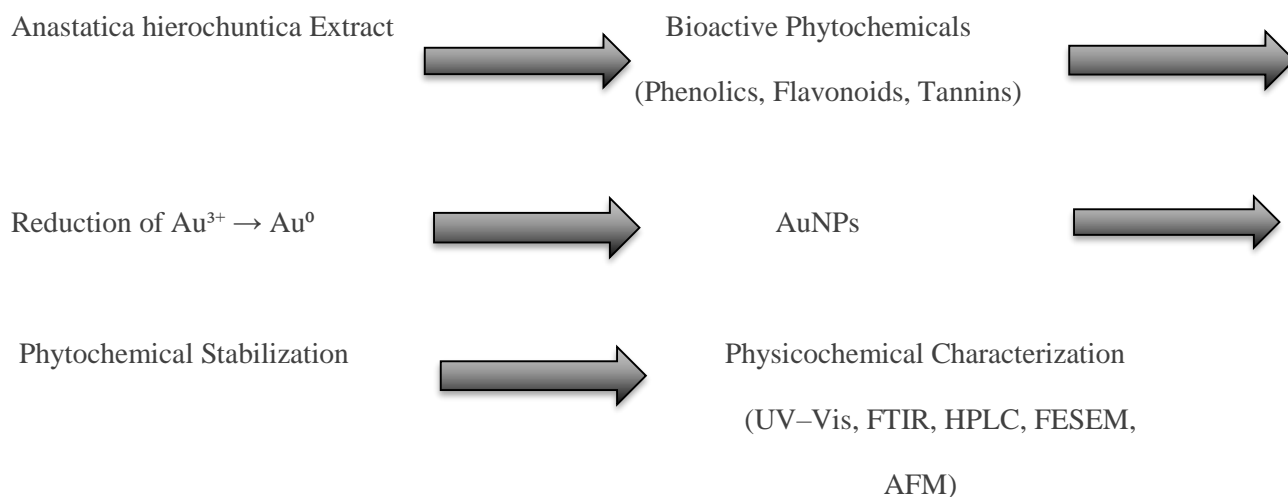
Despite its well-documented medicinal and phytochemical importance, the use of *A. hierochuntica* in the green synthesis of gold nanoparticles has received limited attention. Therefore, investigating this plant as a reducing and stabilizing agent may contribute to expanding the range of plant-based materials

employed in sustainable nanotechnology and provide insights into the synthesis of biocompatible gold nanoparticles with desirable physicochemical characteristics¹⁵.

Materials and Methods

Study design and sample collection:

To investigate the therapeutic properties of *Anastatica hierochuntica* as a plant material, a sample was collected from the western and southern desert of Iraq. Upon collection, the samples were brought to the laboratory collage of Agriculture in Al-Qasim green university while ensuring strict aseptic measures to avoid contamination. The phytochemical screening was carried out to determine the bioactive constituents of the plant.



Plant material extraction:

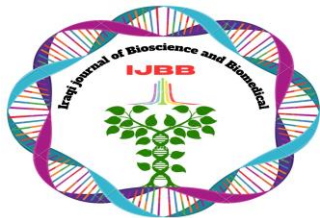
The aqueous plant extract of *Anastatica hierochuntica* is made following the methodology used by Ramazzina et al. (2022) by washing the plant parts with water well to remove contaminants from the surface and drying them well with dry air for three days. 50 grams of whole plant are ground and placed in a glass beaker (capacity 500 ml) Contains (250 ml) of deionized water. The extract was filtered after shaking the mixture at 45°C for 24 hours using Whatman No. 1 filter paper and stored at 4°C until needed.

Preparation of AuCl₄ solution

A concentration (1mM) of gold chloride solution was prepared using the following equation:

$$M(M) = \frac{W(g)}{M.wt(g/mol)} \times \frac{1000}{V(mL)}$$

A 1 mM solution of gold (III) chloride trihydrate (HAuCl₄·3H₂O) was prepared by dissolving 0.0232 g in 100 mL of deionized water¹⁶.



Biosynthesis of gold nanoparticles Au NPs (green synthesis)

Gold nanoparticles were synthesized using an extract of *Anastatica hierochuntica* as a biological reducing and stabilizing agent. Briefly, 20 mL of 1 mM chloroauric acid (HAuCl_4) solution was added dropwise to 100 mL of the aqueous plant extract under constant magnetic stirring.

The reaction mixture was maintained at 45°C for 3 h with continuous stirring at 500 rpm. Formation of AuNPs was initially indicated by a visible color change from pale yellow to ruby red or purple-red, suggesting the reduction of Au^{3+} ions into metallic gold nanoparticles (Au^0)¹⁷.

Drying procedure:

The aqueous extract and aqueous of gold nano particles were prepared put in glass petri dishes and placed in an oven at 45°C for 7-10 days for drying. The resulting powder was collected and stored away from light, air, and moisture for future¹⁸.

Characterization of the plant-based green synthesized gold nanoparticles:

The plant-based green synthesized gold nanoparticles characterization was carried out using All the examination carried out in Phi Nano-Science Center in Baghdad / Al-Karrada/ Al-Senaa Street.

- **Atomic force microscope (AFM):** was used to determine the surface morphology, determine, size and roughness of the prepared gold nanoparticles, a small drop of sample solution was placed on a 1x1 cm glass slide and left to dry at room temperature and ready for testing according to¹⁹.
- **Ultraviolet-visible spectrometer:** A sample was taken within 48 hrs after the preparation of the green nanoparticles and was examined with a UV spectrometer in wavelength range between 200-1000 nm and deionized distilled water was used as blank, where the optical properties of the product were examined at room temperature²⁰.
- **Field emission scanning electron microscopy (FE-SEM):** Fe-SEM-mapping electronic scanner was used to determine the shape and particle size in the prepared samples by placing approximately 5 microliters of ready-to-examine solutions on a mixed gold and carbon electron microscope holder clip, leaving them at room temperature to dry and testing them using different magnifying forces²¹.
- **Energy -dispersive X-ray spectroscopy (EDX):** The sample should be stable under vacuum; stability is only required while the sample chamber is being evacuated since the rest of the analysis is conducted under vacuum to eliminate any atmospheric interference with the electron beam or X-rays. Ideally, the surface should also be clean since X-ray spectroscopy is mostly a near-surface

technique; it should mainly analyze the intended material. For accurate quantitative measurements, the sample should be as thin as possible possible²².

High performance liquid chromatography (HPLC):

A SYKAM HPLC system (Germany) with a C18-ODS column (250 × 4.6 mm, 5 μm) was used for the analysis. The system was injected with 100 μL of samples. The mobile phase was a gradient program of 95% acetonitrile + 0.01% Trifluoroacetic acid for solvent A and 5% acetonitrile + 0.01% Trifluoroacetic acid for solvent B at a flow rate of 1 mL/min. The gradient program used was as follows: 10% A from 0–5 min; 25% A from 5-7 min; 40% A from 7–13 min; and returning to the initial conditions. Detection of phenolic compounds was UV-Visible. detector at 278 nm²³.

Results and discussion

Results in figure 1. shows the changes in extract plant *Anastatica hierochuntica* color to reddish brown from yellow after the reduction reaction with gold chloride during 3h under stirring. It is considered first indicator for green synthesis of gold nanoparticles from the aqueous extract of *Anastatica hierochuntica* the presence of strong reducing phytochemicals in the plant extract not only promotes a fast reduction rate, but act as a capping agent for the green manufacture of nanoparticles.



Figure1 : Steps and color profile change of the aqueous extract of *Anastatica hierochuntica* after addition of gold chloride

This result was on line of those obtained by Moosavy *et al.* (2023)²⁴ who reported that Au NPs was successfully synthesized by using *Mentha spicata* essential oil as demonstrated by the color change of the reaction medium to ruby-red. Also, Wang *et al.* (2020)²⁵ concluded that with the increased concentration of HAuCl₄ addition, the color of the lignin-AuCl₄ suspension turned red which is due to the SPR effect of the green synthesized Au-NPs.

Atomic force microscope (AFM)

The Atomic Force Microscopy (AFM) analysis elucidates a distinct topographical and morphological transformation following the biogenic synthesis of gold nanoparticles (AuNPs) using the *Anastatica hierochuntica* extract.

The preliminary morphological profiling of the crude plant extract (figure 2) showed a relatively low particle density of 1,858,085 particles/mm², together with a mean particle diameter of 64.74 nm and a mean projected area of 7367 nm². The resultant histogram showed a broader and more heterogeneous size distribution, indicating the probable existence of larger aggregates of phytoconstituents or secondary metabolite complexes within the inherent matrix of the plant.

On the other hand, the morphological features of the synthesized AuNPs (see figure 3) show a drastic change that confirms the successful reduction and stabilization at the nanoscale. The average particle diameter has reduced significantly to 42.23 nm, while the mean area has decreased to 3590 nm². At the same time, there has been a remarkable increase in both total particle counts and spatial density, now at 3,119,047 particles/mm², which would indicate the proliferation of various nanostructures. The histogram for the AuNP sample shows a clear shift towards the left, meaning that there is higher frequency of smaller, nearly uniform particles mostly within the range of 20-50 nm as compared to the raw extract.

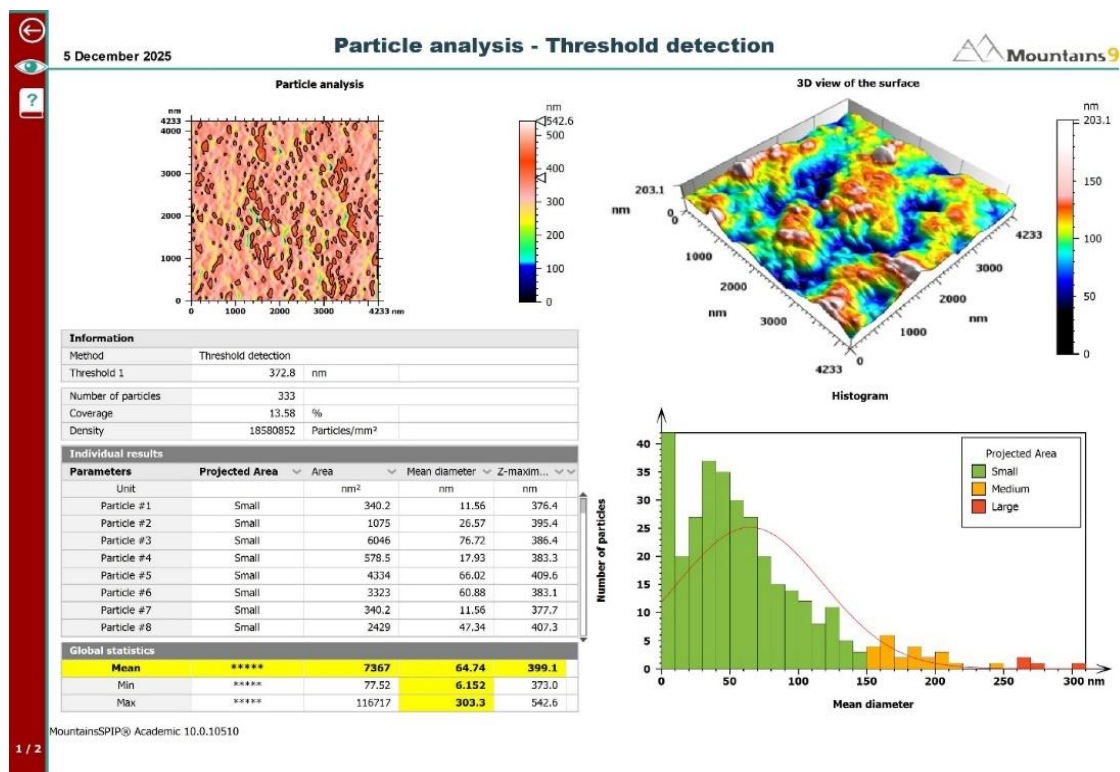


Figure 2. 3-Dimensional and 2-Dimensional image of the surface morphology for the extract using Atomic Force Microscopy (AFM).

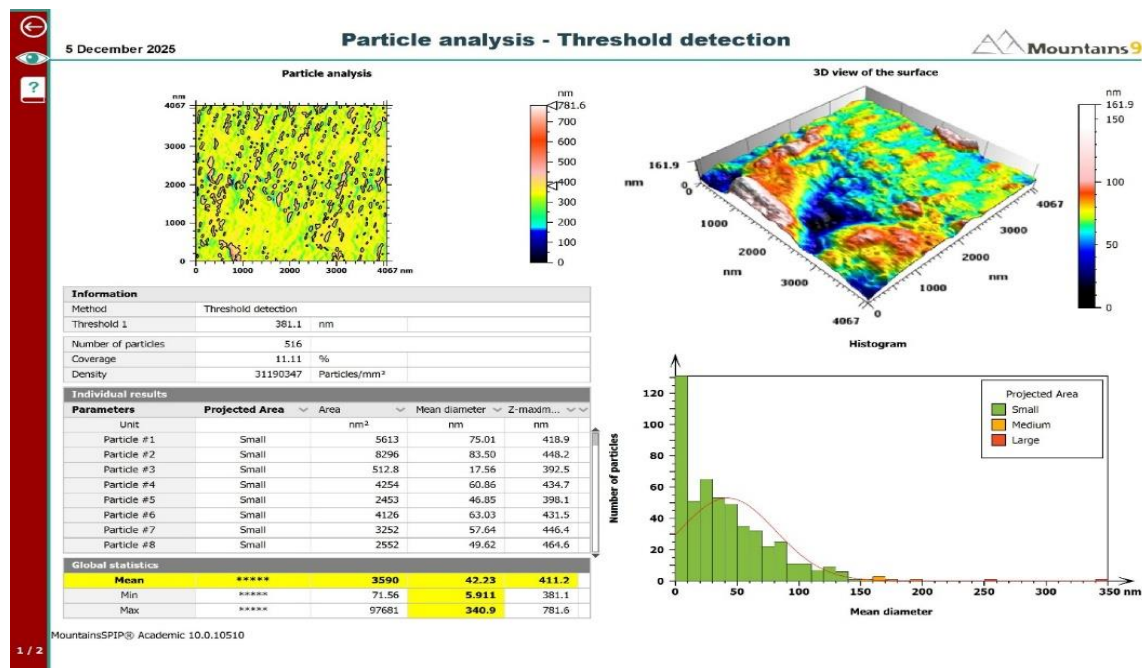


Figure 3. 3-Dimensional and 2-Dimensional image of the surface morphology for the green synthesized AuNPs from the extract using Atomic Force Microscopy (AFM).

This morphological evolution strongly validates the efficacy of *Anastatica hierochuntica* use as both a reducing and capping agent in green nanotechnology. The large, irregular structures in the pure extract function as the biological templates and electron donors that reduce gold ions (Au^{3+} to Au^0). During the nucleation and growth steps, the phytochemicals (e.g., flavonoids, phenols, or terpenoids) cap the newly formed gold clusters. This mode of capping checks great particle agglomeration since it leads to very dense, small, and rather uniformly distributed gold nanoparticles as seen in the second AFM micrograph. The reduction in average particle size together with increased particle density validates the successful bottom-up synthesis and stabilization of AuNPs through bioactive compounds of the plant.

These results were on the line of those obtained by Jehad *et al.* (2022)²⁶ who reported that the AFM study is used to showcase surface features and find topography. The (AFM) gives a 3D image of the surface of a nanoparticle at microscopic resolution. The averaged nano-scale particle diameter equal to the 41.39 nm that illustrates the 2- and 3-dimensional images for synthesized AuNPs' by reduction of $HauCl_4$ with *M. communis* L extract.

Aljabali *et al.* (2018)²⁷ reported that the AuNPs were also prepared using *P. Atlantica* leaves extract at room temperature. AuNPs was prepared with high reaction rate (1min) and was featured by SEM, XRD, EDX and AFM. AuNPs was in 40–50 nm range.

UV-Visible nanoparticles analysis

The UV-Vis absorption spectra provide conclusive optical evidence regarding the successful biogenic synthesis of gold nanoparticles mediated by the *Anastatica hierochuntica* plant extract. The UV-Vis profile of the crude plant extract shows strong absorption only in the ultraviolet region, with major peaks and shoulders observed between 200 nm and 300 nm, notably around 230 nm and 280 nm in figure 4.

This profile has a close similarity to organic phytoconstituents such as polyphenols, flavonoids, and water-soluble proteins, which relate to electronic transitions of aromatic rings and carbonyl groups secondary to those of the plant. The raw extract, importantly, shows very little absorption in the visible light region between 400 nm and 900 nm. However, after the extract has reacted with the gold precursor solution figure 5, a very big change in the optical profile is seen where there is a sharp absorption in the visible region with two strong peaks at about 400 nm and 490 nm. The appearance of this strong absorption band is the clear optical signature of collective coherent oscillations of conduction band electrons on the surface, a phenomenon known as Surface Plasmon Resonance, which confirms the successful bio reduction of trivalent gold ions to metallic gold nanoparticles.

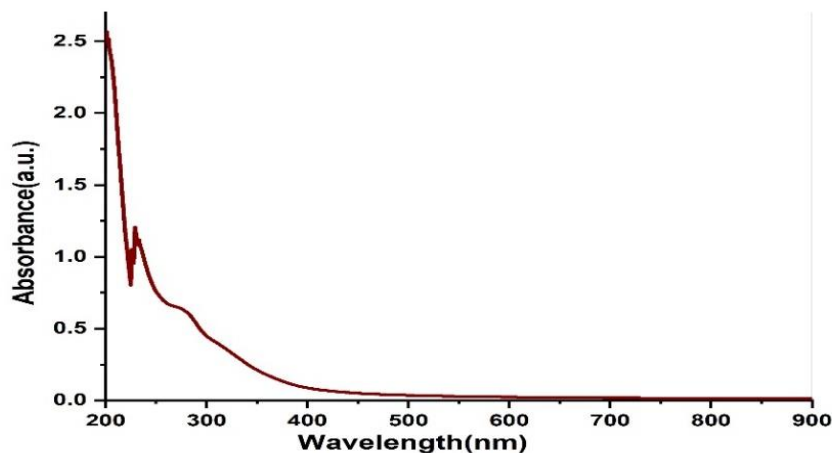


Figure 4: UV-Visible spectroscopy of the crude *Anastatica hierochuntica* plant extract

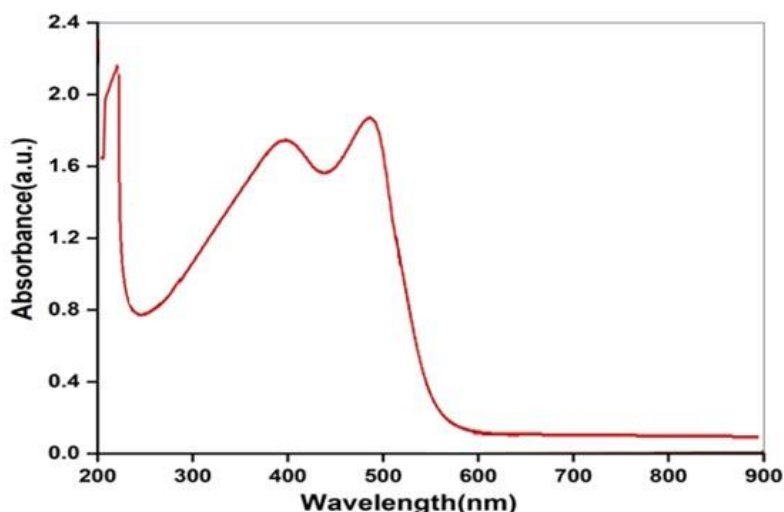


Figure 5: UV-Visible spectroscopy of biosynthesized AuNPs from crude extract

This transition from a purely ultraviolet-active profile in the raw extract to a strongly visible-active profile in the nanoparticle solution demonstrates the dual role of *Anastatica hierochuntica* as a reducing and stabilizing agent. The biomolecules which are responsible for the initial absorption bands in the ultraviolet region act as electron donors. They reduce the gold ions to metallic nuclei. A steady reduction in these plant values confirms their active participation. The specific position and shape of the Surface Plasmon Resonance band strongly depend on nanoparticle size, shape, and capping architecture. The relatively sharp absorption peak located at 490 nm would indicate the formation of small monodisperse or near-spherical gold nanostructures, very consistent with the particle size analysis data. The secondary feature near 400 nm may indicate quantum confined ultra-small clusters or complexation electronic states resulting from the interaction between the nanoparticle surface and the capping of the plant. biomolecules²⁸. The complete exhaustion of the precursor ions and the stabilization of the resonance band highlight the high efficiency and stability of this green synthesis pathway²⁹.

FE-SEM nanoparticle analysis

The Field Emission Scanning Electron Microscopy (FE-SEM) micrographs provide direct visual confirmation of the structural and morphological evolution during the green synthesis of gold nanoparticles AuNPs using *Anastatica hierochuntica* extract.

The surface morphology, spatial arrangement, and dimensional characteristics of the *Anastatica hierochuntica* the description of plant extract and biogenically synthesized gold nanoparticles (AuNPs) was performed successfully using Field Emission Scanning Electron Microscopy (FE-SEM). In Figure 6, it can be seen that the crude plant extract shows a complex, well-defined network of interconnected tubular or nano-fibrous structures. These organic matrices have a smooth surface topography, with fiber diameters ranging from 97.8 nm to 128.12 nm, acting as highly porous scaffolding with high surface area abundant in reductive functional groups.

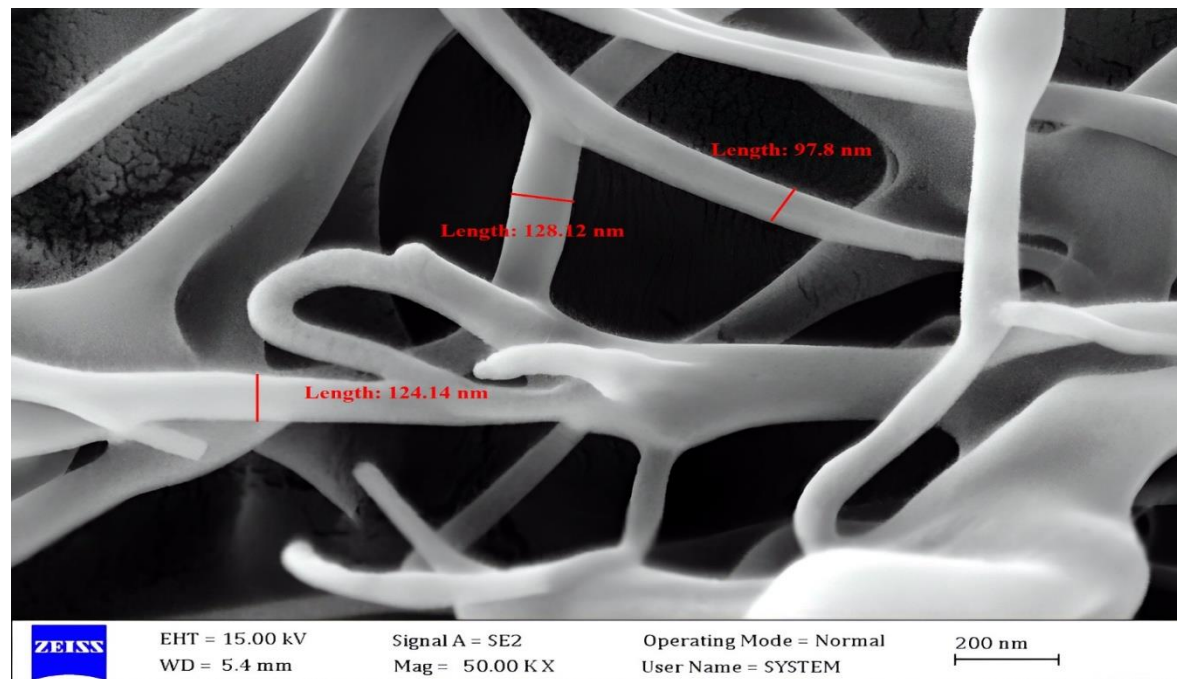


Figure 7: FE-SEM micrograph of crude *Anastatica hierochuntica* plant extract showing the native interconnected fibrous network.

The introduction of the gold precursor Au^{3+} leads to a deep morphological transformation as observed in figure 7. The fibrous architecture serves as a sacrificial template and stabilizing matrix to facilitate the nucleation and isotropic growth of highly dense, distinct spherical to quasi-spherical gold nanostructures. The AuNPs synthesized are of uniform distribution over the biomolecular surface exhibiting ultrafine particle sizes measured predominantly between 20.46 nm and 48.29. This drastic reduction in size and change to a granular, spherical nano-morphology strongly relates to the UV-Vis SPR data obtained earlier and the mean topological diameters (42.23 nm) from AFM. The analysis by FE-SEM shows conclusively that the phytochemical constituents within the *Anastatica hierochuntica* network effectively restricted spatial particle growth and prevented detrimental nano-agglomeration, successfully yielding monodisperse and structurally stable metallic nanoparticles.

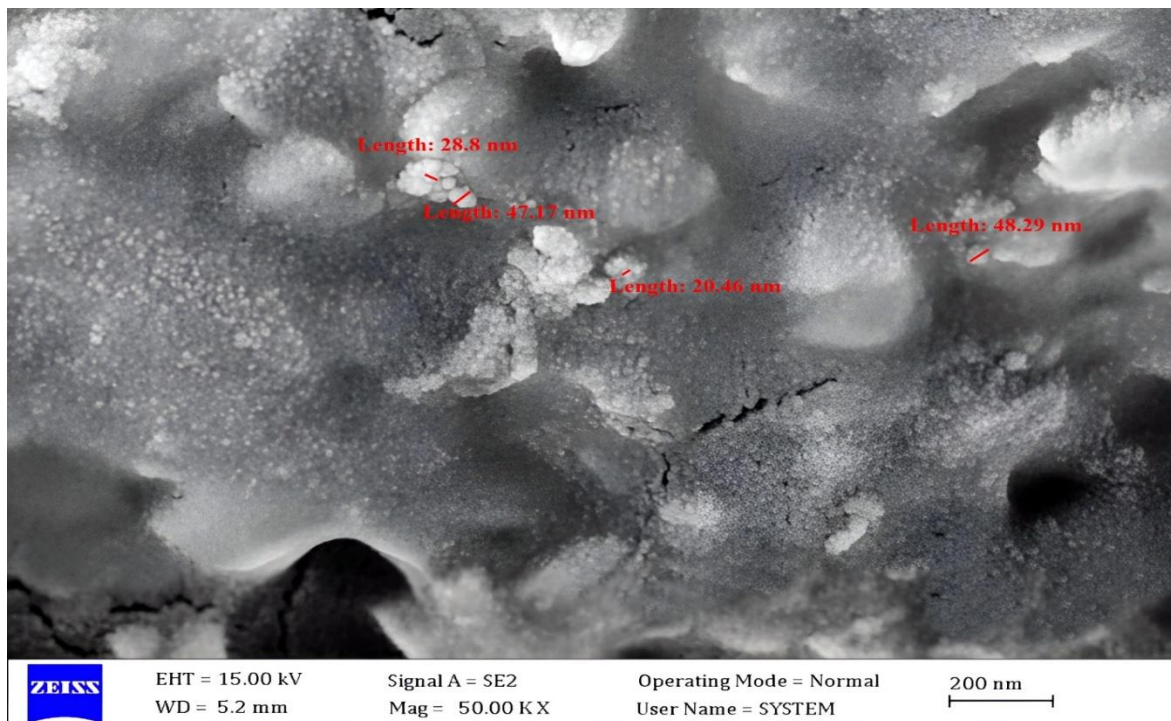


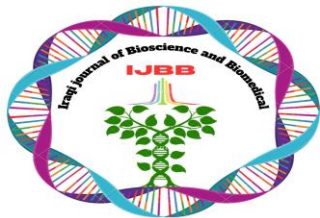
Figure 7: FE-SEM micrograph of biogenically synthesized gold nanoparticles (AuNPs) using *Anastatica hierochuntica* extract.

High performance liquid chromatography (HPLC):

High Performance Liquid Chromatography was used to compare the main phenolic and flavonoid compounds in the raw water extract of *Anastatica hierochuntica* and the remaining liquid after making gold nanoparticles. The exact amounts of these active components are shown in Table 1.

The examination of the unprocessed plant extract revealed that Gallic acid was the predominant compound, measured at 142.6 ppm, with Rutin closely following at 120.1 ppm. The subsequent compounds were identified in a descending order: Quercetin at 98.7 ppm, Ferulic acid at 81.6 ppm, Caffeic acid at 71.4 ppm, and p-coumaric acid at 63.2 ppm. Luteolin exhibited the lowest concentration at 52.9 ppm. The graph of the extract showed distinct and pronounced peaks that matched very well with the standard reference materials.

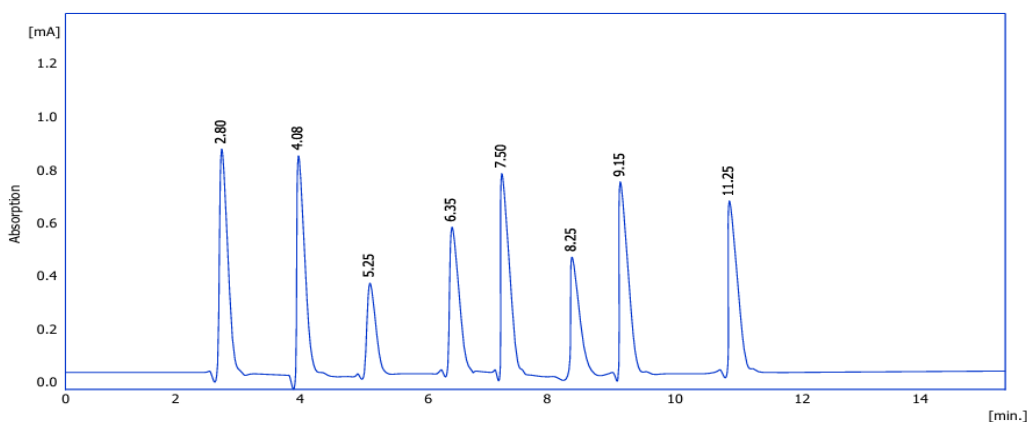
After the green synthesis of gold nanoparticles, there was remarkable and general reduction in the concentrations of all the plant compounds under study. Gallic acid reduced significantly from 142.6 ppm to 95.0 ppm; Rutin and Quercetin went down sharply to 71.4 ppm and 63.0 ppm, respectively. The most substantial relative reductions were registered by Luteolin and p-coumaric acid, which lost over fifty percent of their initial concentrations and ended up at 18.0 ppm and 24.1 ppm, respectively.



Chemically, it can be argued that the apparent reduction showed that these phenols and flavonoids were responsible for the nanoparticles' formation. The steady decrease in values proves that these molecules were electron donors, reducing the gold ions to stable metallic gold nanoparticles. Simultaneously, the other parts of these molecules capped the surface of the newly formed nanoparticles. This duality of reduction and coating played a significant role in controlling the size of the particles to the very small dimensions observed in the images taken by electron microscopy and atomic force microscopy and also preventing agglomeration of the nanoparticles.

Table 1. Concentration of the main phenolic and flavonoid compounds in parts per million for the *Anastatica hierochuntica* plant extract and the gold nanoparticle sample.

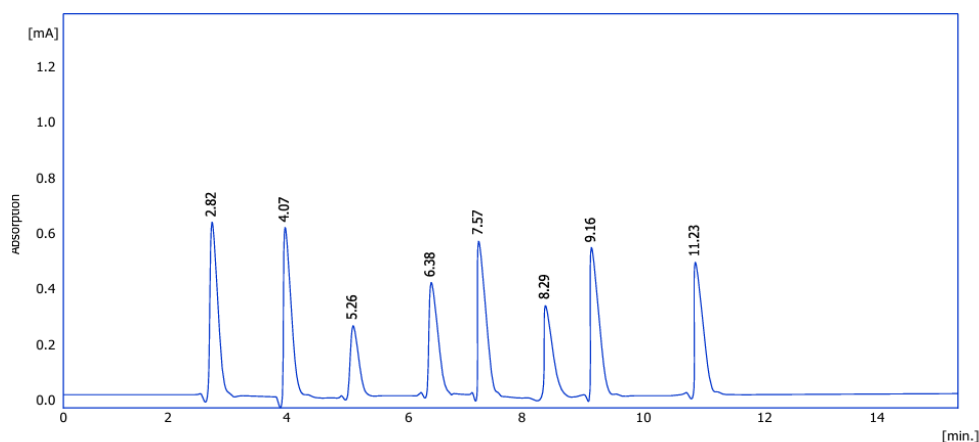
No	Name (PPM)	Extract	Nano
1	Caffeic acid	71.4	33.2
2	Ferulic acid	81.6	50.2
3	Gallic acid	142.6	95.0
4	Luteolin	52.9	18.0
5	p-coumaric acid	63.2	24.1
6	Quercetine	98.7	63.0
7	Rutin	120.1	71.4



Result chromatography Table (Uncal - F:\ sample extract)

No	Reten. Time [min]	Area [mAU.s]	Height [mAU]	Area [%]	Height [%]	W05 [min]	Compound Name
1	2.80	8952.65	844.14	16.00	16.00	0.15	
2	4.08	8477.11	830.25	16.00	16.00	0.15	
3	5.25	2365.98	369.80	8.00	8.00	0.05	
4	6.35	3698.57	547.14	11.00	11.00	0.08	
5	7.50	6541.14	711.45	13.00	13.00	0.13	
6	8.25	3625.41	433.21	10.00	10.00	0.10	
7	9.15	4568.74	710.32	13.00	13.00	0.13	
8	11.25	4123.66	650.14	13.00	13.00	0.13	
	Total	42353.69	5069.15	100.00	100.00		

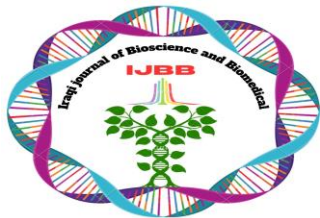
Figure 8. HPLC chromatogram and peak integration data table of the crude *Anastatica hierochuntica* plant extract showing the initial baseline areas of polyphenolic compounds.



Result chromatography Table (Uncal - F:\ sample nano)

No	Reten. Time [min]	Area [mAU.s]	Height [mAU]	Area [%]	Height [%]	W05 [min]	Compound Name
1	2.82	5214.05	611.25	16.00	16.00	0.15	
2	4.07	5011.65	601.12	16.00	16.00	0.15	
3	5.26	1041.14	221.45	8.00	8.00	0.05	
4	6.38	2033.54	345.98	11.00	11.00	0.08	
5	7.57	4874.17	426.58	13.00	13.00	0.13	
6	8.29	1320.44	266.65	10.00	10.00	0.10	
7	9.16	1698.89	421.11	13.00	13.00	0.13	
8	11.23	1885.08	401.32	13.00	13.00	0.13	
	Total	23078.47	3295.47	100.00	100.00		

Figure 9. HPLC chromatogram and peak integration data table of the gold nanoparticle sample showing the reduced peak areas after the green synthesis reaction.



Thotathil *et al.*, (2023)¹⁵ carried out a phytochemical analysis of *Anastatica hierochuntica* Grown in Qatar to identify its active ingredients and evaluate its biological activities, it was found that the plant is highly rich in active components, including specific flavonoids and phenolic acids which give the water extract strong antioxidant properties. These findings regarding the rich chemical profile of this plant support our current results, confirming that these abundant phytochemicals were the main components consumed during the nanoparticle creation.

Another study by Suthar *et al.*, (2017)³² employed liquid chromatography as a significant means to divide and define gold nanoparticles from gold auric chloride starting materials. They determined that gold auric chloride elutes at a retention time of 2 minutes, while the coated gold nanoparticles elute later at a retention time of 2.7 minutes. Their results for chromatographic separation are highly consistent with our HPLC data since the clear change in peak positions confirmed successful transformation of the gold starting materials.

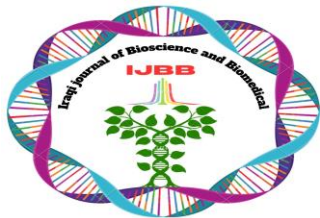
Additionally, a related study by Kim *et al* (2026)³³ studied the intracellular distribution and conversion of gold nanoparticles within cancerous MCF-7 cells using mass spectrometry techniques. They confirmed that the gold nanoparticles were structurally stable in the cytosol of the cell and did not degrade into ionic forms of gold. These results vary somewhat from our present emphasis because they tested the nanoparticles inside living cancer cells, but their findings of stability agree with our observation that the plant coating does indeed protect the gold nanoparticles.

Conclusions

The present study successfully demonstrated the green synthesis of gold nanoparticles (AuNPs) using the aqueous extract of *Anastatica hierochuntica* as a natural reducing and stabilizing agent. The formation of AuNPs was initially confirmed by the characteristic color change of the reaction mixture and subsequently verified through UV–Visible spectroscopy. Further characterization using FTIR, HPLC, FE-SEM, AFM, and EDX analyses revealed the involvement of plant-derived phytochemicals in nanoparticle synthesis, confirmed the presence of elemental gold, and provided information regarding the morphology, surface characteristics, and physicochemical properties of the synthesized nanoparticles. The results indicate that *A. hierochuntica* extract can serve as an effective and environmentally friendly alternative for the synthesis of gold nanoparticles without the use of hazardous chemicals. The synthesized AuNPs exhibited physicochemical characteristics consistent with those reported for plant-mediated gold nanoparticles. However, the biological activities and potential biomedical applications of these nanoparticles were not investigated in the present study and therefore require further evaluation through appropriate *in vitro* and *in vivo* studies. Overall, this work contributes to the growing field of green nanotechnology by demonstrating the feasibility of utilizing *A. hierochuntica* extract for the sustainable synthesis of gold nanoparticles.

Acknowledgments

I would like to express my gratitude to my supervisor for the immense help and support she provided me with during the practical work of this project. Her direct supervision and hands-on support



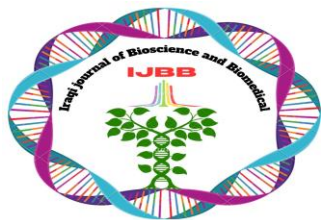
were very important for the successful completion of the experimental task. Her insightful comments and advice in the field of science helped to remove the problems and sharp comments and advice in the field of science helped to remove the problems and assure that this research was completed as good and effective as possible.

Author's Declaration

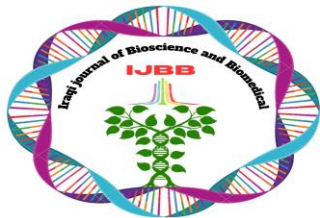
We so attest that every table in the document is exclusive and was made by us.

References

1. Abdullah, M., Obayedullah, M., Shariful Islam Shuvo, M., Abul Khair, M., Hossain, D., & Nahidul Islam, M. (2025). A review on multifunctional applications of nanoparticles: Analyzing their multi-physical properties. *Results in Surfaces and Interfaces*, 21, 100635.
2. Khan, I., Saeed, K., Ali, N., Zada, N., Khan, A., & Ali, F. (2020). Micro and Nano Technologies.
3. Atroshi, F., Westermarck, T., Kaipainen, P., Selga, G., Sauka, M., & Aboltina, L. (2014). Pharmacological and Clinical Effectiveness of *Zingiber officinale* and *Alpinia galanga* in Patients with Osteoarthritis. In F. Atroshi (Ed.), *IntechOpen*.
4. Wanjari, A. S., & Wanjari, D. S. (2019). An Overview on Herbal Medicine. *International Journal of Research in Pharmaceutical Sciences*, 11(1), 14–17.
5. Veenadevi, A., Sree, K. D., Lohitha, G., Shankar, N. U., & Babu, P. S. (2024). Combining Herbs for Enhanced Efficiency: A Conceptual Guide to Polyherbal Formulation. 12(12), 242–253.
6. Hassanisaadi, M., Bonjar, G. H. S., Rahdar, A., Pandey, S., Hosseinipour, A., & Abdolshahi, R. (2021). Environmentally Safe Biosynthesis of Gold Nanoparticles Using Plant Water Extracts. *Nanomaterials*, 11(8).
7. Perveen, K., Husain, F. M., Qais, F. A., Khan, A., Razak, S., & Afsar, T. (2021). Microwave-Assisted Rapid Green Synthesis of Gold Nanoparticles Using Seed Extract of *Trachyspermum ammi*: ROS Mediated Biofilm Inhibition and Anticancer Activity. *Biomolecules*, 11(2).
8. Leng, G., Duan, B., Liu, J., Li, S., Zhao, W., & Wang, S. (2024). The advancements and prospective developments in anti-tumor targeted therapy. *Neoplasia*, 56, 101024.
9. Zhou, T., Maimait, K., Xu, H., & Pan, L. (2026). A Comprehensive Characteristic of *Anastatica hierochuntica*.
10. Baker, R. K., Ali, B. H., & Jameel, N. M. (2013). The Effect of Aqueous Extract of *Anastatica hierochuntica* on Some Hormones in Mouse Females. 26(2), 198–205.
11. Sussich, F., Skopec, C., Brady, J., & Cesàro, A. (2001). Reversible Dehydration of Trehalose and Anhydrobiosis: From Solution State to an Exotic Crystal? *Carbohydrate Research*, 334(3), 165–176.
12. Rostan, N. A. S. (2024). Traditional Uses and Pharmacological Properties of *Anastatica hierochuntica*. 11(June), 67–78.
13. Md Zin, S. R., Kassim, N. M., Mohamed, Z., Fateh, A. H., & Alshawsh, M. A. (2019). Potential Toxicity Effects of *Anastatica hierochuntica* Aqueous Extract on Prenatal Development of Sprague-Dawley Rats. *Journal of Ethnopharmacology*, 245, 112180.



14. Dizaye, K., Alchalabi, D. A., & Marouf, B. H. (2023). Effects of Flaxseed (*Linum usitatissimum*) on Postmenopausal Symptoms and its Clinical Parameters. *32*, 257–265.
15. Thotathil, V., Sidiq, N., Fakhroo, A., & Sreerama, L. (2023). Phytochemical Analysis of *Anastatica hierochuntica* and *Aerva javanica* Grown in Qatar: Their Biological Activities and Identification of Some Active Ingredients. *Molecules*, *28*(8), 3364.
16. Wijesuriya, N. (2021). For How Long Can a Prepared 1 mM H₂AuCl₄ Solution Be Used?
17. Mardina, V., Fadlly, T. A., Harmawan, T., Sufriadi, E., Iqramullah, M., & Umar, H. (2024). Green Synthesis of Gold Nanoparticles from the Aqueous Extracts of *Sphagneticola trilobata* as Anti-Breast Cancer Agents. *Journal of Advanced Pharmaceutical Technology & Research*, *15*(2), 75–80.
18. Ali, M. M., Mohammed, A., Ali, M. M., & Ali, F. F. (2020). Synthesis of Gold Nanoparticles by Using Batch Method and Study its Antibacterial Activity. *17*(2).
19. AlShaheeb, Z. A., Oraibi, A. G., & Thabit, Z. A. (2023). Effect of Green-Biosynthesis Aluminum Nanoparticles (Al NPs) on *Salmonella enterica* Isolated from Baghdad City. *Baghdad Science Journal*, *20*, 1840–1857.
20. Asif, M., Yasmin, R., Asif, R., Ambreen, A., Mustafa, M., & Umbreen, S. (2022). Green Synthesis of Silver Nanoparticles (AgNPs), Structural Characterization, and Their Antibacterial Potential. *Dose-Response*, *20*(1).
21. Robles-Gómez, L., Sáez-Espinosa, P., & Gómez-Torres, M. J. (2025). Field Emission Scanning Electron Microscopy (FE-SEM) as an Approach for Membrane Surface Mapping in Cell Biology. *Methods in Molecular Biology*, *2897*, 435–444.
22. Cotutela, T. I. N. (2019). Design, Development, and Characterization of Thin Film Filters for High Brilliance Sources in the EUV–Soft X-Ray Spectral Range.
23. Schieppati, D. (2019). Experimental Methods in Chemical Engineering: High Performance Liquid Chromatography (HPLC).
24. Moosavy, M. H., de la Guardia, M., Mokhtarzadeh, A., Khatibi, S. A., Hosseinzadeh, N., & Hajipour, N. (2023). Green Synthesis, Characterization, and Biological Evaluation of Gold and Silver Nanoparticles Using *Mentha spicata* Essential Oil. *Scientific Reports*, *13*(1), 7230.
25. Wang, B., Yang, G., Chen, J., & Fang, G. (2020). Green Synthesis and Characterization of Gold Nanoparticles Using Lignin Nanoparticles. *Nanomaterials*, *10*.
26. Rahee, S. S., & Jehad, R. H. (2023). Comparing the Effectiveness of Using Three Different Re-Mineralizing Pastes on Remineralisation of Artificially Induced White Spot Lesion. *Journal of Baghdad College of Dentistry*, *35*(4), 35–45.
27. Aljabali, A. A. A., Akkam, Y., Al Zoubi, M. S., Al-Batayneh, K. M., Al-Trad, B., & Abo Alrob, O. (2018). Synthesis of Gold Nanoparticles Using Leaf Extract of *Ziziphus zizyphus* and Their Antimicrobial Activity. *Nanomaterials*, *8*(3).
28. Peng, S., McMahon, J. M., Schatz, G. C., Gray, S. K., & Sun, Y. (2010). Reversing the Size-Dependence of Surface Plasmon Resonances. *Proceedings of the National Academy of Sciences of the United States of America*, *107*(33), 14530–14534.
29. Pechyen, C., Tangnorawich, B., Toommee, S., Marks, R., & Parcharoen, Y. (2024). Green Synthesis of Metal Nanoparticles, Characterization, and Biosensing Applications. *Sensors International*, *5*, 100287.



30. Dwivedi, A. D., & Gopal, K. (2010). Biosynthesis of Silver and Gold Nanoparticles Using *Chenopodium album* Leaf Extract. *Colloids and Surfaces A: Physicochemical and Engineering Aspects*, 369(1), 27–33.
31. Hadi, I. S., & Yas, R. M. (2022). Gamma Radiation Effect on Characterizations of Gold Nanoparticles Synthesized Using Green Method. 63(10), 4305–4313.
32. Suthar, J. K., Rokade, R., Pratinidi, A., & Kambadkar, R. (2017). Purification of Nanoparticles by Liquid Chromatography for Biomedical and Engineering Applications. 617–624.
33. Kim, J., Bae, C., Hernández Millares, R., Kim, T., Lee, Y., & Lee, K. (2026). Time-Point-Based Analysis of Gold Nanoparticles in MCF-7 Cells Following Ultrasound Irradiation: Quantitative and Label-Free Intracellular Characterization. *Nanoscale Advances*, 8(8), 2787–2798.